



Article

Characterization, Expression Profiling, and Biochemical Analyses of the *Cinnamoyl-CoA Reductase* Gene Family for Lignin Synthesis in Alfalfa Plants

Weiti Cui ^{1,†}, Zihan Zhuang ^{1,†}, Peihao Jiang ¹, Jincheng Pan ¹, Gan Zhao ¹, Sheng Xu ² and Wenbiao Shen ^{1,*} 

¹ Laboratory Center of Life Sciences, College of Life Sciences, Nanjing Agricultural University, Nanjing 210095, China; wtcui@njau.edu.cn (W.C.); z15298388017@163.com (Z.Z.); phjiang216@163.com (P.J.); 2018216034@njau.edu.cn (J.P.); 2018216033@njau.edu.cn (G.Z.)

² Institute of Botany, Jiangsu Province and Chinese Academy of Sciences, Nanjing 210014, China; xusheng@cnbg.net

* Correspondence: wbsenh@njau.edu.cn; Tel.: +86-25-84396542

† These authors contributed equally to this work.

Abstract: *Cinnamoyl-CoA reductase* (CCR) is a pivotal enzyme in plant lignin synthesis, which has a role in plant secondary cell wall development and environmental stress defense. Alfalfa is a predominant legume forage with excellent quality, but the lignin content negatively affects fodder digestibility. Currently, there is limited information on CCR characteristics, gene expression, and its role in lignin metabolism in alfalfa. In this study, we identified 30 members in the CCR gene family of *Medicago sativa*. In addition, gene structure, conserved motif, and evolution analysis suggested *MsCCR1–7* presumably functioned as CCR, while the 23 *MsCCR-like*s fell into three categories. The expression patterns of *MsCCRs/MsCCR-like*s suggested their role in plant development, response to environmental stresses, and phytohormone treatment. These results were consistent with the *cis*-elements in their promoters. Histochemical staining showed that lignin accumulation gradually deepened with the development, which was consistent with gene expression results. Furthermore, recombinant *MsCCR1* and *MsCCR-like1* were purified and the kinetic parameters were tested under four substrates. In addition, three-dimensional structure models of *MsCCR1* and *MsCCR-like1* proteins showed the difference in the substrate-binding motif H212(X)2K215R263. These results will be useful for further application for legume forage quality modification and biofuels industry engineering in the future.

Keywords: *cinnamoyl-CoA reductase*; kinetic analysis; lignin biosynthesis; *Medicago sativa*



Citation: Cui, W.; Zhuang, Z.; Jiang, P.; Pan, J.; Zhao, G.; Xu, S.; Shen, W. Characterization, Expression Profiling, and Biochemical Analyses of the *Cinnamoyl-CoA Reductase* Gene Family for Lignin Synthesis in Alfalfa Plants. *Int. J. Mol. Sci.* **2022**, *23*, 7762. <https://doi.org/10.3390/ijms23147762>

Academic Editor: Azzurra Stefanucci

Received: 22 June 2022

Accepted: 12 July 2022

Published: 14 July 2022

Publisher's Note: MDPI stays neutral with regard to jurisdictional claims in published maps and institutional affiliations.



Copyright: © 2022 by the authors. Licensee MDPI, Basel, Switzerland. This article is an open access article distributed under the terms and conditions of the Creative Commons Attribution (CC BY) license (<https://creativecommons.org/licenses/by/4.0/>).

1. Introduction

Alfalfa (*Medicago sativa* L.) is a worldwide-cultivated legume forage, with high nutrition and good palatability [1]. Digestibility is part of the key indicators of forage quality, which has a significant influence on animal performance. Generally, forage digestibility is affected by various cellular components, including lignin content [2]. Genetically reducing lignin content in forage legumes can improve digestibility and animal performance, as well as commercialization for forage quality improvement [3]. For example, the *caffeic acid O-methyltransferase* downregulated transgenic tall fescue plants showed reduced lignin content and significantly increased digestibility [4]. When fed adult horses with reduced lignin alfalfa hay, an improvement in the dry matter digestibility was found, with no change in forage consumption, fecal particle size, or digesta retention time [5]. By using transgenic alfalfa lines with downregulated cytochrome P450 enzymes in lignin pathway, it showed a strong negative relationship between lignin content and rumen digestibility but not between lignin composition and digestibility [6]. However, it is difficult to draw a conclusion on whether the changes in lignin monomer could benefit biomass digestibility because there is a lack of unified research background in the previous studies [7]. In

addition, lignin also has a negative impact on the conversion of lignocellulose biomass into cellulosic ethanol in the biofuels production industry [8–10]. Interestingly, alfalfa is considered a potential feedstock for biofuels due to its being valuable in lignocellulosic biomass [11]. Thus, lignin content modification is an important strategy for both forage and biofuel engineering, with no effect on the plant yield [12].

Lignin is a group of polyphenolic polymers that are deposited predominantly in the thickened secondary cell walls [13]. The evolution of lignin was accompanied by the emergence of the vascular land plants and exhibited both distinct subcellular localization and monomeric composition in specific cell types [14]. Plants with loss-of-function of genes in lignin biosynthesis, such as *cinnamoyl-CoA reductase* (CCR), generally showed collapsed xylem and/or dwarf phenotype [15]. Moreover, lignification is one of the responses of plant cells to various environmental stresses. There is a close relationship between lignin accumulation and environmental stresses in many plant species. For example, in different Iranian cultivars of basil, water deficit stress leads to increasing expression of genes in lignin synthesis [16]. Under copper (Cu^{2+}) stress condition, *Panax ginseng* suspension cultures showed an increased accumulation of phenolics and lignin, which reflects the protective response to Cu^{2+} -induced cell damage [17]. During the plant-environment interaction, the functional integrity of the plant cell needs the maintenance of cell wall integrity. Stresses-induced cell wall damage could initiate the secondary reactive oxygen species (ROS) burst and jasmonic acid (JA) accumulation, followed by a negative feedback loop that represses each other's production and subsequent lignin accumulation [18]. In addition, lignin content and the expression of lignin-metabolism-related genes were found to play critical roles in lodging resistance of common buckwheat and barley [19,20]. Interestingly, genetically modified plants with decreased lignin biosynthesis can indirectly influence the synthesis of other secondary metabolites and the expression of stress-related genes [21].

Lignin is synthesized in the spaces between the cell wall polysaccharides by the oxidative coupling of three monolignols, coniferyl alcohol, sinapyl alcohol, and *p*-coumaryl alcohol, and then there is incorporation into lignin to form guaiacyl (G), syringyl (S), and *p*-hydroxyphenyl (H) subunits, respectively [14,22]. In plants, lignin monomers are synthesized from phenylalanine in the cytoplasm by two of a total of three branches. The first branch, which is called the general phenylpropanoid pathway, is from phenylalanine to *p*-coumaroyl-CoA and subsequent feruloyl-CoA. This pathway is shared with some important secondary metabolites, such as flavonoids and coumarins [23,24]. The second branch is called monolignol pathway, in which hydroxycinnamoyl-CoA esters are reduced by CCR (EC 1.2.1.44) and cinnamyl alcohol dehydrogenase (CAD; EC 1.1.1.195) to generate monolignols [25]. CCR catalyzes the *p*-coumaryl-CoA, caffeoyl-CoA, and feruloyl-CoA to form *p*-coumaraldehyde, caffeoyl aldehyde, and coniferaldehyde, respectively, and is further converted to the corresponding monolignols, coumaryl alcohol, caffeoyl alcohol, and feruloyl alcohol, with the CAD catalyst [14]. Common to all three branches of the lignin synthesis pathway, genetic changes of CCR and CAD genes tend to exhibit overall reduced lignin content but not one or two monomer(s) [7,26,27]. Therefore, CCR is a pivotal enzyme involved in monolignols biosynthesis in plants.

The CCR gene family exhibits diversity in different plant species. Two CCR genes and five CCR-like genes were found in *Arabidopsis thaliana*. *AtCCR1* plays a role in lignification during the plant developmental stage, and *AtCCR2* is functionally expressed in stress and pathogen response [28,29]. The mutant of *AtCCR1* exhibits decreased lignin content, while triple mutant with the loss-function of *CAD-C*, *CAD-D*, and *CCR1* contains 50% of wild-type lignin content and shows a severe dwarf phenotype and male sterility [30]. Reintroduced *CCR1* expression specifically in the protoxylem and metaxylem vessel cells in the mutant of *AtCCR1* can effectively overcome the vascular collapse and stem biomass yield decrease, regardless of the similar cell wall composition and metabolome compared with *AtCCR1* mutation plants [31]. In switchgrass, *PvCCR1* and *PvCCR2* were found to possess CCR activity, whereas *PvCCR1* might function in lignin biosynthesis during development stage

and *PvCCR2* might be involved in stress defense [32]. In *Populus trichocarpa*, Shi et al. [33] identified 11 CCRs, and *PtrCCR2* showed high expression in differentiating xylem and significantly less in other tissues. In model legume *Medicago truncatula*, Zhou et al. [34] have identified two CCR genes, in which *MtCCR1* had a critical effect on plant growth, while *MtCCR2* exhibited moderate reduced lignin content and little influence on growth phenotype. In rice, the *OsCCR* knockdown plants showed a decrease in lignin deposition in root and anther. Interestingly, a component of an SCF E3 ligase *OsFBK1* mediated *OsCCR* degradation, suggesting the role of *OsFBK1* and *OsCCR* in the development of rice anthers and roots [35]. However, there is still little knowledge of the characteristics of the CCR family genes that respond to lignin biosynthesis in widely cultivated forage *M. sativa*.

Cultivated alfalfa is an autotetraploid ($2n = 4x = 32$), so it generates a lot of trouble in the identification of its genes and molecular genetic research. Recently, alfalfa (*M. sativa* L.) genome sequencing has been completed, in which it was reported with 3010 Mb of genome size [36]. This provides a great opportunity for the genome-wide analysis of the CCR gene family. In this study, we searched the alfalfa genome database to identify CCR family members and further analyzed the gene structures, evolutionary relationships, and gene expression patterns. Finally, we cloned and further recombinantly expressed *MsCCR1* and *MsCCR-like1*, followed by the kinetic parameters and three-dimensional structure analysis, to explore the *MsCCR*s protein structure and possible function in lignin biosynthesis.

2. Results

2.1. Identification and Analysis of Cinnamoyl-CoA Reductase (CCR) Genes in *M. sativa* Genome

In total, 30 putative CCR gene sequences were identified from *M. sativa* genome database by domain confirmation and homology research with the signature motif KN-WYCYGK. Among them, 7 CCR genes were identified with full-length CCR motif sequences, and 23 sequences with partial CCR motifs were characterized as *CCR-like* genes (Table S1). Of the 23 *CCR-like* genes, 7 *CCR-like* genes (namely *MsCCR-like1–7*) are homologous to *M. truncatula CCR-like* genes *SNL6-1/2*, and the other 16 *CCR-like* genes (namely *MsCCR-like8–23*) are homologous to *MtCCR1-3/4*. The molecular weight of 30 predicted *MsCCR*/*MsCCR-like* proteins varied from 32.35 to 39.85 kDa, with isoelectric points (pI) in the range of 5.00–7.48.

2.2. Gene Structure, Evolution, and Conserved Motif Analysis of *MsCCR*s/*MsCCR-like* Genes

To find out evolutionary relationships among members of the CCRs from alfalfa, a neighbor-joining (N-J) tree was constructed based on the nucleotide sequences (Figure 1A). The 30 *MsCCR*s/*MsCCR-like*s sequences were divided into 5 subfamilies, and subfamily I contained all 7 *MsCCR* genes, while *MsCCR-like* genes were classified in subfamilies II–V (Figure 1A). Furthermore, the intron/exon structure of *MsCCR*s/*MsCCR-like* genes was shown (Figure 1B). It can be clearly seen that genes in the same subfamily have similar gene structures. In turn, there are distinct differences in gene structures among the different subfamilies, with the different numbers of introns from 2–5. For example, subfamily IV has 2 introns, subfamily V has 5 introns, and most of the CCR genes (subfamilies I, II, and III) contain 4 introns. By using the MEME online software, 20 conserved motifs in the *MsCCR*s were captured, and further analyses were carried out (Figure 1C). Furthermore, the sequence of each motif was analyzed (Table S2). All of the *MsCCR*/*MsCCR-like* proteins contain motifs 1–6. Proteins in groups I, IV, and V contain motifs 7 and 9, while proteins in groups I and V contain motif 8. Furthermore, proteins in groups I and V mainly lack the motifs 11–13, 15, 19, and 20. In addition, motifs 18, 15, 20, and 16 are unique to proteins in groups I, III, IV, and V, respectively.

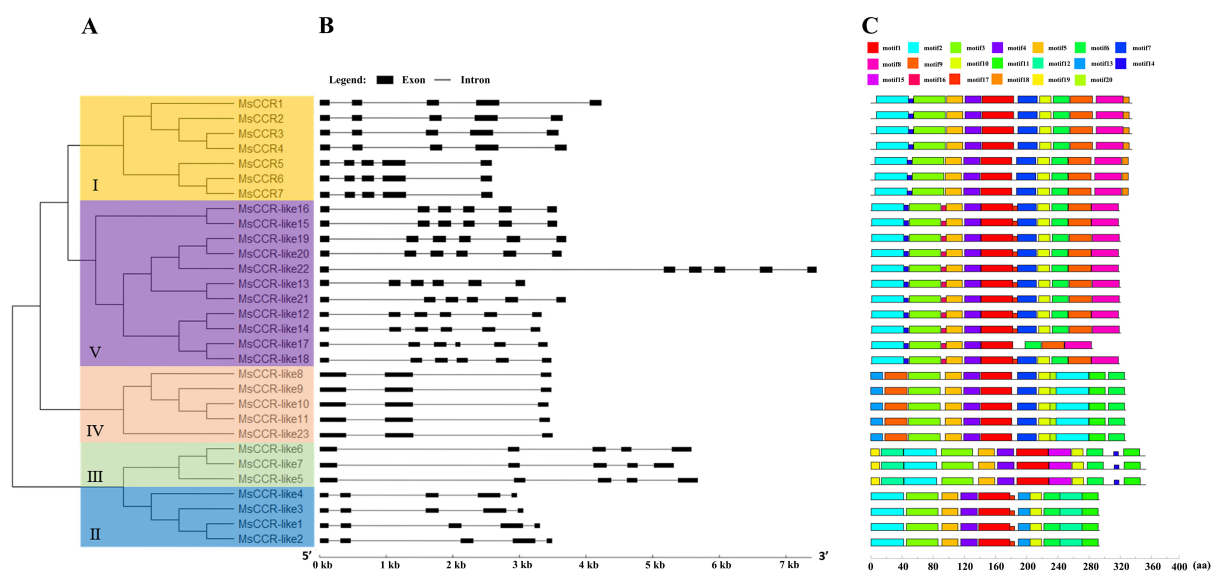


Figure 1. The gene structures and conserved motifs of MsCCR and MsCCR-likes based on evolutionary relationships. Phylogenetic relationships of MsCCR and MsCCR-like genes (A). The exon-intron structure of MsCCR and MsCCR-like genes (B). Distribution of putative conserved motifs in MsCCR and MsCCR-like proteins (C).

We further constructed two phylogenetic trees with CCRs in alfalfa and other plants to clarify their relationships and predict the possible biological functions (Figure 2). Three CCR-like genes and 19 CCR genes from different plants, including *M. truncatula*, *Arabidopsis thaliana*, *Oryza sativa*, *Zea mays*, *Triticum aestivum*, *Solanum tuberosum*, *Trifolium pretense*, *Leucaena leucocephala*, *Eucalyptus gunnii*, *Pinus radiata*, *Picea abies*, and *Populus trichocarpa*, were selected from NCBI [37] (Table S3). All CCRs/CCR-like proteins fell into two groups: the CCR bona fide clade and the CCR-like clade. For example, all the 23 MsCCR-like proteins and one AtCCR-like protein as well as two MtCCR-like SNLs were clustered into the CCR-like clade, and the others were parceled into the CCR bona fide clade. The CCR bona fide clade was further classified into three subfamilies: dicot clade, monocot clade, and gymnosperm clades, and 7 MsCCRs were clustered together with LlCCR1, EgCCR, AtCCR1/2, PtCCR, PtrCCR, and PbCCR1 (Figure 2A). Furthermore, many identified CCRs with the function related to lignin biosynthesis exhibit a close relationship to MsCCRs (in Group I) in the radiation tree (Figure 2B). These results indicated possible functional diversity between CCR and CCR-like proteins.

The chromosome distribution of CCRs in *M. sativa* and *M. truncatula* was further analyzed to study the evolutionary mechanism of the CCR gene family. MsCCR1, MsCCR2, MsCCR3, and MsCCR4 were distributed on *M. sativa* chromosome 2.1, 2.2, 2.3, and 2.4, respectively, which were paired with MtCCR1 on *M. truncatula* chromosome 2. MsCCR5, 6, and 7 were distributed on *M. sativa* chromosome 4.1, 4.2, and 4.3, respectively, which were paired to MtCCR1-2 on *M. truncatula* chromosome 4 (Table S1, Figure S1A). While, MsCCR-likes were distributed on *M. sativa* chromosomes 2.1, 2.2, 2.3, 2.4, 4.1, 4.2, 4.3, 4.4, 8.2, 8.3, 5.1, 5.2, 5.3, 5.4, 6.1, 6.2, and 6.3, which were linked to MtCCR1-3, MtCCR1-4, MtCCR-like SNL6, and MtCCR-like SNL6-2 on *M. truncatula* chromosome 2, 4, 5, and 6, respectively (Table S1, Figure S1B).

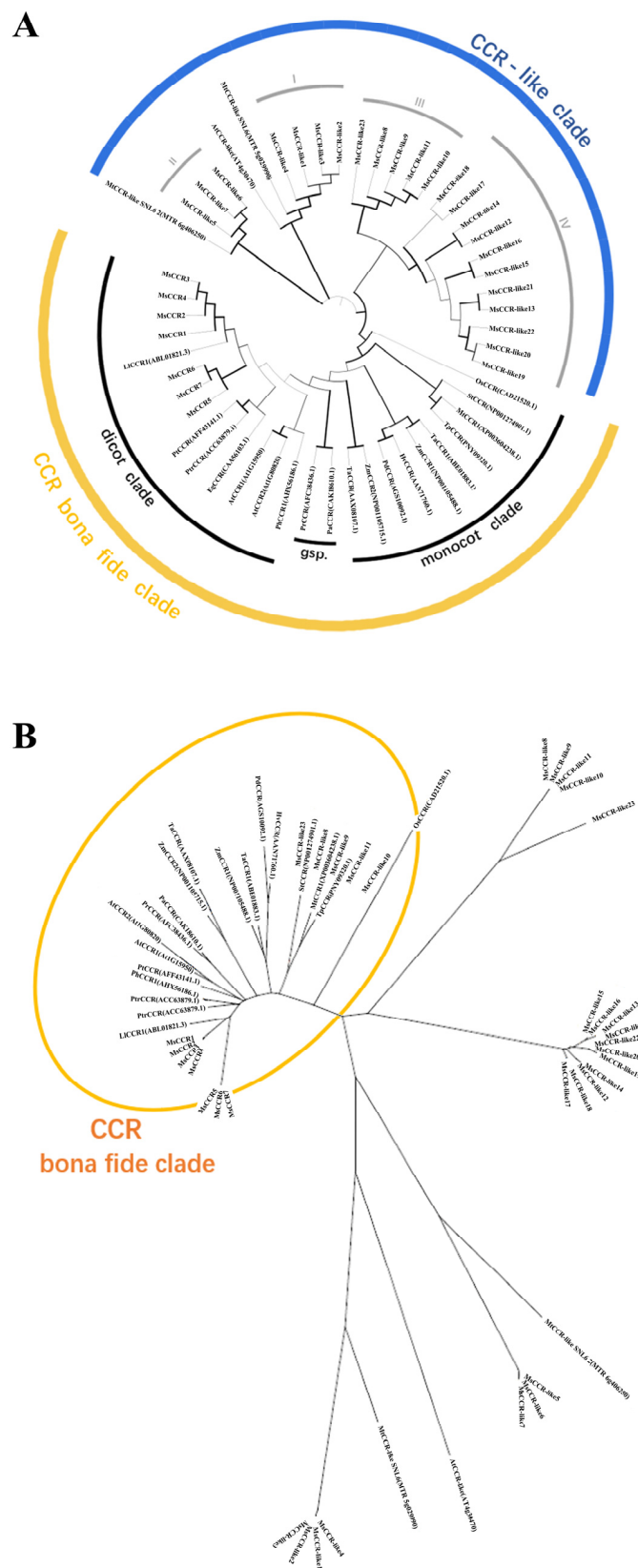


Figure 2. The phylogenetic analysis of CCR proteins across various plants. Traditional phylogenetic tree (A) and radiation tree (B) of 30 CCR protein sequences from *M. sativa* and 22 CCR protein sequences from other species. Protein sequences were constructed using MRGA-X software based on the neighbor-joining (NJ) method. The species name and the accession number of sequences used to construct the phylogenetic tree are listed in Table S3.

2.3. The Cis-Acting Regulatory Elements in the Promoter of MsCCRs

The regulation of gene expression in organ cells is a complex process, and transcriptional activation of promoters is a vital event. The promoter of *MsCCR*/*MsCCR-like* genes contained a variety of *cis*-acting elements, including ABRE, ARE, BOX4, G-Box, GT1-motif, MYB, and MYC (Figure 4). For example, the promoters of *MsCCR1–4* have light-related *cis*-acting elements (GT1-motif, Box4, and G-Box), ARE, as well as MYB- and MYC-binding elements, suggesting the expression of *MsCCR1–4* might be involved in light stimulus, anaerobic induction, stress response, and plant development [39]. The elements in promoters of *MsCCR5–7* are comparable, mainly including MYC, Box4, and MYB. Many of the promoters of *MsCCR-like*s possess the elements related to plants responding to stress, such as MYB, MYC, ABRE, ARE, and Box4. These data indicate that *MsCCRs*/*MsCCR-like*s might participate in plant response to numerous stresses or development-related phytohormone.



Figure 4. The putative *cis*-elements and transcription factor binding sites in the promoter regions of *MsCCR* and *MsCCR-like* genes. The colored blocks represent different types of *cis*-acting elements and their locations in each *MsCCR*/*MsCCR-like* gene.

2.4. The Expression Patterns of *MsCCR*/*MsCCR-like* Genes and Lignin Content Analysis during Different Growth Stage

RT-qPCR was then performed to examine the role of *MsCCR*/*MsCCR-like* genes in alfalfa during different developmental stages. According to the specificity of CDS sequences, 6 pairs of specific primers were obtained, for example, Group Ia (*MsCCR1–4*), Group Ib (*MsCCR5–7*), Group IV (*MsCCR-like8–11, 23*), Group III (*MsCCR-like5–7*), Group II (*MsCCR-like1–4*), and *MsCCR-like17*. As shown in Figure 5A, the transcripts of *MsCCR1–4* (Group Ia) were upregulated, especially in the shoot after 28 days of growth. Meanwhile, the transcripts of *MsCCR5–7* (Group Ib) did not change considerably, with higher levels underground than aboveground. Unexpectedly, transcripts of genes in Group IV showed more abundance than Group Ia, and increased expression with the development process was also shown. In addition, the expression pattern of genes in Group III was similar to Group Ib, and Group II was similar to Group Ia. The transcript of *MsCCR-like17* exhibited slight induction, especially in leaves. Meanwhile, histochemical staining was employed to explore the lignin levels in the alfalfa plant stem and root. The coloration gradually deepened with the development process, especially after 28 days of growth.

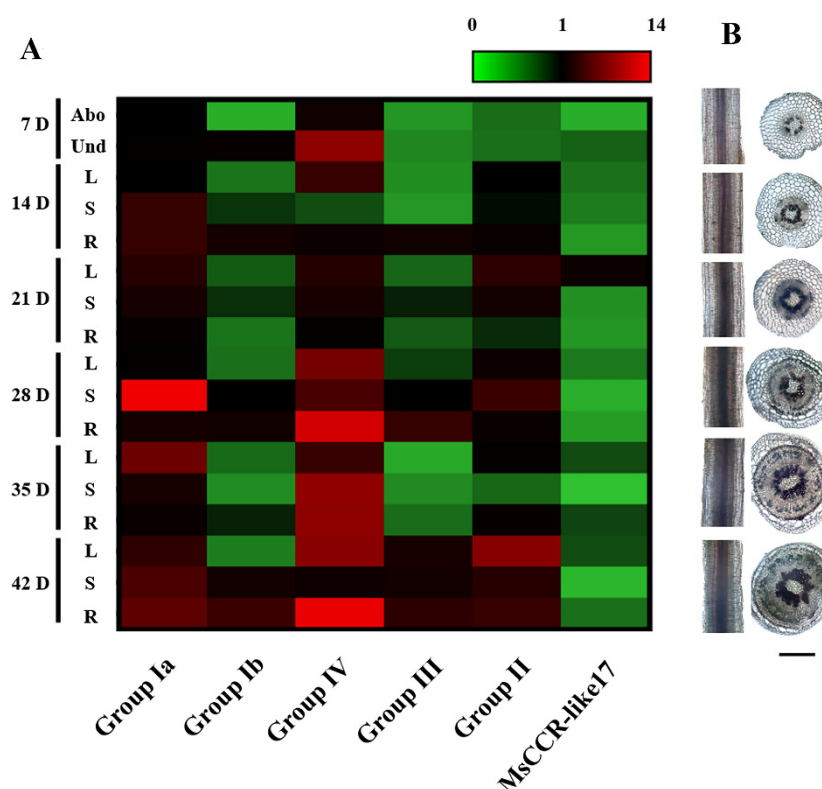


Figure 5. The expression profiles of *MsCCR/MsCCR-like* genes in different tissues at 1–6 weeks of different growth period. Gene expression (A) and phloroglucinol histochemical staining (B) were analyzed at different parts after 7, 14, 21, 28, 35, and 42 days (D) of growth. Data were from three independent experiments with at least three replicates for each. *Actin2* was used as internal reference, and the relative expression of each gene was further compared to the sample of the above ground part after 7 days of growth. Abo: above ground; Und: underground; L: leaf; S: stem; R: root. Bar = 1 mm.

2.5. The Expression Patterns of *MsCCRs/MsCCR-likes* under Abiotic Stresses and Hormone Treatment

Further experiments were performed to detect the response of *MsCCR/MsCCR-like* genes under various stresses and hormone treatments. As shown in Figure 6A, with cold (4 °C), NaCl, PEG6000, AlCl₃, and CdCl₂ treatment, the transcript levels of genes in Group Ia and Group II were slightly increased at early (1 h) and late stage (48 h), but downregulated (especially under Al stress) at 6 and 24 h of treatment. Meanwhile, the transcripts of genes in Group Ib and Group III showed a similar trend but it was more obvious under 4 °C and NaCl treatments. The genes in Group IV were mainly induced at 3–24 h with 4 °C and NaCl treatments, and there was strong induction at 1–3 h and reduction at 48 h. The transcript of *MsCCR-like17* showed decreased expression after 3–24 h of 4 °C, NaCl, PEG6000, AlCl₃, and CdCl₂ treatments. After 1 h of ultraviolet-B (UV-B) treatment and subsequent recovery period, genes in Group Ia/Ib/II/III were upregulated, while *MsCCR-like17* and genes in Group IV showed a downregulated trend during stress treatment and recovery periods.

After exogenous salicylic acid (SA) treatment, the transcripts of genes in Group Ia/Ib/III were slightly upregulated at 6 h but decreased after 24 h of treatment (Figure 6B). The abscisic acid (ABA), nitric oxide donor sodium nitroprusside (SNP), and ethephon (ETH) treatments showed similar trends with the upregulated expression of genes in Group Ia/Ib/II at the late stage (48 h) of treatment. The genes in Group III showed a downregulated trend before 24 h of ABA, SNP, and ETH treatment but were upregulated after 48 h of treatments. In addition, the transcripts in Group IV were increased during the first 24 h but decreased after 48 h of SA, ABA, and SNP treatments, and they showed an obvious

decrease at the 3 h point of the ETH treatment. While the expression of *MsCCR-like17* was enhanced at the late stage (24–48 h) of treatment.

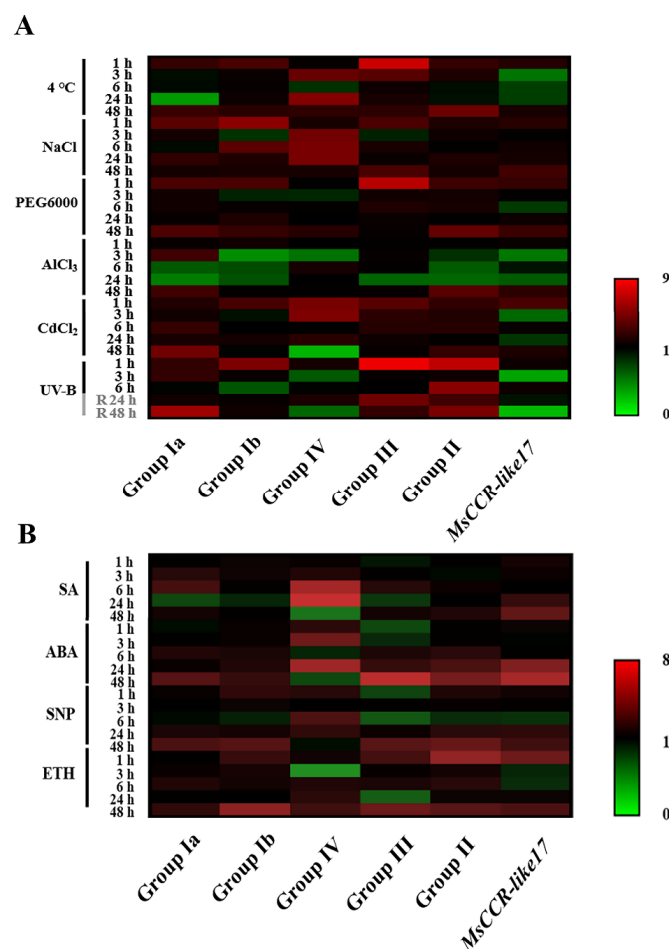


Figure 6. The expression profiles of *MsCCR*/*MsCCR-like* genes under different treatments and different times in *M. sativa*. Seven-day-old alfalfa seedlings were used for abiotic stresses (A) and phytohormone (B) treatment. After 1, 3, 6, 24, and 48 h of 4 °C, NaCl (100 mM), PEG6000 (15%), AlCl₃ (150 μM), CdCl₂ (100 μM), SA (50 mg/L), ABA (50 mg/L), SNP (80 μM), and ETH (500 μM) treatment, the transcripts were analyzed by RT-qPCR. UV-B (1 J·m⁻²·h⁻¹) was treated for 6 h, followed by 12 h of recovery (in grey). Data were from three independent experiments with at least three replicates for each. *Actin2* was used as internal reference, and the relative expression of each gene was further compared to control samples at the same time point under each treatment.

2.6. Cloning, Heterologous Expression, and Enzymatic Assay of *MsCCR1* and *MsCCR-like1* Gene

To illustrate the biochemical functions of *MsCCRs*, we cloned *MsCCR1* (in Group I) and *MsCCR-like1* (in Group II) gene. Heterologous expression of the His-tagged *MsCCR1* and *MsCCR-like1* was successfully obtained from *E. coli* by 0.2 mM isopropyl-β-D-thiogalactopyranoside (IPTG) induction at 16 °C. Recombinant *MsCCRs* were purified with Ni²⁺ affinity chromatography, followed by molecular masses analysis through SDS-PAGE. The molecular masses of the *MsCCR1* exhibited about 37.21 kDa, and *MsCCR-like1* was about 33.61 kDa, which is consistent with their theoretical molecular mass (Figure S2).

Furthermore, the kinetic parameters of recombinant *MsCCR1* and *MsCCR-like1* to different substrates, including feruloyl-, *p*-coumaroyl-, caffeoyl-, and sinapoyl-CoAs, were investigated, respectively. As shown in Table 1, *MsCCR1* catalyzed feruloyl-CoA, *p*-coumaroyl-CoA, and sinapoyl-CoA, but it had the lowest Michaelis constant value (*K_m*) for sinapoyl-CoA. In addition, the catalytic efficiency (*K_{cat}*/*K_m*) of *MsCCR1* for sinapoyl-CoA was more than twice that for feruloyl-CoA and *p*-coumaroyl-CoA. Correspondingly,

MsCCR-like1 catalyzed *p*-coumaroyl-CoA and caffeoyl-CoA, with similar K_m and K_{cat}/K_m . The different characters in catalyzing suggest their diverse functions in lignin synthesis.

Table 1. Kinetic analysis of MsCCR1 and MsCCR-like1.

| Symbols | Feruloyl-CoA | | <i>p</i> -Coumaroyl-CoA | | Caffeoyl-CoA | | Sinapoyl-CoA | |
|-------------|------------------|---------------|-------------------------|---------------|----------------|---------------|----------------|---------------|
| | K_m | K_{cat}/K_m | K_m | K_{cat}/K_m | K_m | K_{cat}/K_m | K_m | K_{cat}/K_m |
| MsCCR1 | 45.20 ± 11.42 ab | 2.09 ± 0.18 B | 24.22 ± 4.51 bc | 2.58 ± 0.11 B | ND | ND | 10.57 ± 1.25 c | 5.72 ± 0.36 A |
| MsCCR-like1 | ND | ND | 44.14 ± 7.12 ab | 1.09 ± 0.19 C | 48.16 ± 1.75 a | 1.09 ± 0.11 C | ND | ND |

K_m : Michaelis constant (μM); K_{cat}/K_m : catalytic constant/Michaelis constant ($\mu\text{M min}^{-1}$); “ND”: not detectable. Data are mean ± SE of three independent experiments. Different letters indicate significant differences at $p < 0.05$ according to Duncan’s multiple range test.

2.7. Three-Dimensional Structure Analysis of CCRs in *M. sativa* and Other Plants

The three-dimensional structure models of MsCCR1 and MsCCR-like1 proteins in the bona fide clade were constructed (Figure 7A,B). It can be seen that a part of the MsCCR-like1 in the C terminal is missing, which including the substrate-binding motifs H212(X)2K215R263 (Figure 7C,D). Furthermore, three-dimensional structure models of some representative members MsCCR5, MsCCR-like7/11/17/21, and typical CCR protein in other species, including MtCCR, AtCCR1/2, TaCCR2, EgCCR, PtCCR, LlCCR1, ZmCCR2, and PaCCR2, were also constructed (Figure S3). The structures of MsCCR1, MsCCR5, and the identified CCRs in other plants share high similarities, but MsCCR-likes exhibited structural changes within them in some parts of the protein (Figure S4). In addition, the alignment of the above CCR/CCR-like proteins showed that some key amino acid residues are missing in MsCCR-likes compared to CCRs. These results suggest that the catalytic function of the MsCCR-likes might be different from that of MsCCRs.

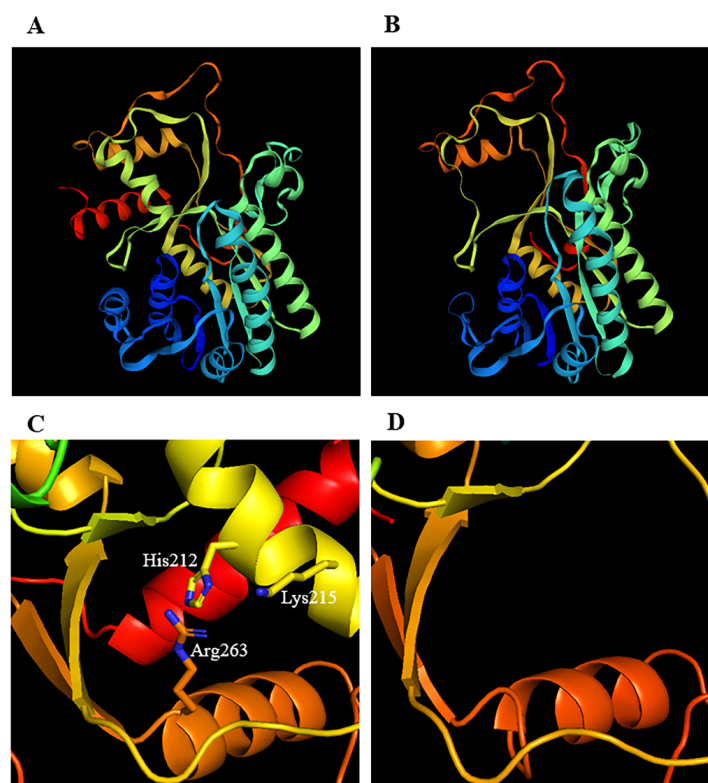


Figure 7. The predicted three-dimensional structure of MsCCR1 (A) and MsCCR-like1 (B), and the detailed structure in the C-terminal end of MsCCR1 (C) and MsCCR-like1 (D). The spirals, arrows, and lines indicate the α -helices, β -sheets, and turns and coils, respectively. The sticks indicate catalytic triads H212(X)2K215R263 with corresponding.

3. Discussion

CCR plays a central role in lignin biosynthesis, and it is considered to be a biotechnological target in lignocellulosic biomass engineering [40]. Meanwhile, it is also the target to decrease lignin content in alfalfa because of its enormous influence on forage digestibility [41]. However, little is known about the CCR gene family in the widely cultivated forage *M. sativa*. In this study, we identified 7 *MsCCR* genes with the location at chromosomes 2.1–2.4 and 4.1–4.3 in *M. sativa* (Figures 1 and S1; Table S1). The proteins encoded by *MsCCR1–4* (with the same protein length and pI) and *MsCCR5–7* (with the same protein length and pI) are homologous to functionally characterized *MtCCR1* and *MtCCR1-2*, respectively (Table S1; [34,42]). The deficiency of the CCR gene in chromosome 4.4 suggested chromosomal fragment loss events during evolution. In addition, we also identified 23 *MsCCR-like*s with partially altered motif KNWYCYGK. The phylogenetic trees showed they are clustered together with a closed relationship to *AtCCR-like* and *MtCCR-like*s (Figure 2).

Diverse CCR gene families have been reported in some plant species. In *Arabidopsis*, 11 putative CCR genes have been identified [43]. In addition, there are 11 CCRs in *Populus tomentosa*, 33 in *Oryza sativa*, 10 in *Eucalyptus grandis*, 31 in pear (*Pyrus bretschneideri* Rehd.), and 9 in *Populus trichocarpa* [7,24,33,44,45]. The CCR member in most diploid plants is almost half in the tetraploid plant such as alfalfa and some diploid plants with whole-genome duplication events such as Chinese white pear. In addition, this is also the reason that there have been many tandem duplication events during alfalfa evolution, which can be concluded from the synteny analysis of *CCR/CCR-like* genes in *M. sativa* and *M. truncatula* (Figure S1).

The *cis*-element predicted in the promoter of *MsCCR/MSCCR-like* genes suggested the involvement of *MsCCR/MSCCR-like* in plant development (MYB/MYC), phytohormone response (ABRE), and stresses response, such as light (GT1-motif), anaerobic induction (ARE), and MYB-involved abiotic stress responses (Figure 4; [46,47]). Further expression profiling showed that *MsCCR1–4* (Group Ia) and *MsCCR-like1–4, 8–11, 23* (Groups II and IV) are mainly involved in lignin synthesis during the development process (Figure 5). The lignin content and CCR gene expression were gradually increased in tobacco during maturation [48]. Similarly, the transcripts of *CsCCR* were raised during the stem development of the tea plant, and they showed higher levels in “Fudingdabai” compared to “Suchazao”, with the results of higher lignin accumulation in “Fudingdabai” compared to “Suchazao” [49]. The transcription of lignin-synthesis-related genes can be regulated by transcript factors such as MYBs [50,51]. However, in the expression of *MsCCR5–7* (Group Ib) and some *MsCCR-like*s (Group III and *MsCCR-like17*), a few changes even decreased during the 28 days of plant development (Figure 5). This may be because of the different *cis*-element in the promoter of these genes compared to that in Group Ia, II, and IV (Figure 4). Interestingly, some researchers argue that not all members of the CCR families are involved in lignin synthesis after a long period of evolution [52].

Meanwhile, the expression of *MsCCR5–7* (Group Ib), *MsCCR-like5–7* (Group III), and *MsCCR-like8–11, 23* (Group IV) was upregulated with varying degrees after chilling, salinity, drought, heavy metals, and UV-B stresses (Figure 6). Several reports have shown that CCR participated in plants coping with environmental stresses. The early response genes to salt stress in the root of melon seedlings include CCR and transcript factor *MYB* [53]. *CCR11* was upregulated under salt and water-deficient conditions in *Populus trichocarpa* [54]. In addition, the expression patterns of *MsCCR1–4* and *MsCCR5–7* were different during development and stress response (Figures 5 and 6). This is consistent with a further report that *CCR1* is involved in lignification during the development process, while *CCR2* is involved in stress responses in *Arabidopsis* [28]. In addition, the loss function of *MtCCR1* showed deficiency in plant growth, but the mutation of *MtCCR2* does not exhibit inhibited plant growth [34,42]. The function of *MsCCR5–7* (homologous to *MtCCR2* in [34]) and most *MsCCR-like*s might be plant defense against biotic and abiotic stresses by regulating

lignin biosynthesis [55,56]. These diverse function and expression profiles of CCRs might be related to their duplication during evolution [57].

The expression of *MsCCRs* and *MsCCR-likes* (in particular) exhibited different induced levels under phytohormone SA, ABA, SNP, and ETH treatments (Figure 6). These findings indicated that CCR participated in phytohormone-mediated development, biotic stress, and abiotic stress responses. For example, the ethylene response factor AP2/ERF Ii049 mediated methyl jasmonate, SA, and ABA response by regulating CCR-associated lignin synthesis [58]. In addition, the expression levels of CCRs after ABA treatment are in accordance with the results of the ABRE element in the promoter of CCRs in alfalfa (Figures 4 and 6). The underlying pathway might include some transcript factors such as MYBs and NACs [23,56,59]. Furthermore, it was found that ETH-treated strawberry showed higher hemicelluloses, cellulose, and neutral sugars than the control [60]. Al-induced pectin and hemicellulose accumulation can be alleviated by SNP treatment in rice root cells [61]. Although the effects of lignin content on stress resistance and feed quality are contradictory, these results suggested the possible role of other composites in the cell walls to solve this contradiction, in other words, with reduced lignin and enhanced resistance.

To further illustrate the functions of the *MsCCRs* and *MsCCR-likes*, we cloned and expressed recombinant *MsCCR1* and *MsCCR-like1*, followed by the biochemical analyses (Table 1; Figure S2). The *MsCCR1* showed catalytic ability with the substrates feruloyl-CoA, *p*-coumaroyl-CoA, and sinapoyl-CoA, which is similar to the findings in *EgCCR*, *AtCCR1*, and *PhCCR1* [62–64]. Meanwhile, the substrates *p*-coumaroyl-CoA and caffeoyl-CoA can be catalyzed by *MsCCR-like1*, suggesting that *MsCCR-likes* also play a role in lignin synthesis. Combined with the promoter analysis and expression profile (Figures 4 and 6), the functions of CCR-like might be linked to plant defense response [65]. Chao et al. [38] point out that H2O2(X)2K205 is a crucial motif that can be used to distinguish between CCRs and CCR-like proteins. In this text, the results from three-dimensional structure models showed the primary difference is the missing of the H212(X)2K215R263 motif and the C-terminal end in *MsCCR-like1* protein (Figure 7), which also can be found in the results of protein alignment (Figure 3). Prasad et al. [1] concluded that the ARG51, ASN52, ASP54, and ASN58 in CCRs are critical residues for feruloyl binding. In this study, the motif RNXD(X)3N is found in *MsCCR1* (NADP specificity box in Figure 3) but not in *MsCCR-like1* (with QQYGEXXX instead). Pan et al. [64] found that residues Ile124, Gly125, Val185, Leu186, Ala220, and Tyr284 formed a *Ph-CCR1* binding pocket for the phenolic ring. The *MsCCR1* is in possession of I134, G135, V195, L196, A206, and Y275 residues, which consist of the reported CCR proteins, but not in *MsCCR-like1* and other *MsCCR-likes* (Figures S3 and S4). These results highlight the potential use of the CCRs in alfalfa genetic engineering, as well as pharmacologic decreased CCR gene expression by specific chemicals. On the contrary, environmental-stresses-induced CCR gene expression might be helpful for plant defense but might have a negative effect on forage quality. Therefore, the overall quality should also be considered when the genetic approach was implemented targeting lignin-reduced plants. Furthermore, it will be very interesting to study the function of CCR-likes and to compare the structural and functional differences between CCR and CCR-like in future work.

4. Materials and Methods

4.1. Plant Growth and Treatments

Sterilized alfalfa seeds (*M. sativa* L. Victoria, Clover Seed & Turf Co., Beijing, China) were germinated at 25 °C for 1 d, and then uniform seeds were selected and transferred to the illuminating incubator in quarter-strength Hoagland's solution [66]. Five-day-old seedlings were used for common environmental stresses and plant hormone treatments. NaCl was used for salinity stress at 100 mM [67]; PEG6000 was used for mimicking drought stress at 15% (*w/v*) [68]; AlCl₃ was used at 150 μM [69]; and CdCl₂ was used at 100 μM [66]. UV-B treatment was performed using the methods described by Xie et al. [70], 1 J·m⁻²·h⁻¹ treated for 6 h and recovered for another 42 h. Salicylic acid (SA) was used at 50 mg/L [71];

abscisic acid (ABA) was used at 50 mg/L [72]; nitric oxide donor sodium nitroprusside (SNP) was used at 80 μ M [61]; and ethephon (ETH) was used at 500 μ M immediately after preparation [60]. All the reagents were purchased from Sigma-Aldrich (St. Louis, MO, USA).

4.2. MsCCR Identification and Classification

For MsCCRs gene determination, a local protein database was established by using DNATOOLS software with alfalfa (*M. sativa* L.) genomic data [36,73]. To identify candidates of the CCR family, sequences of 2 CCRs from *Arabidopsis thaliana* (At1G15950 and At1G80820) and 6 CCRs from *Medicago truncatula* (MTR_2g104960, MTR_4g006940, MTR_5g029990, MTR_6g406250, MTR_2g028620, and MTR_4g009040) were used for BLASTp and BLASTn (E-value \leq 0.001; Identities \geq 80%; obtained from NCBI: www.ncbi.nlm.nih.gov, accessed on 30 April 2021) analysis. When comparing, the single exon similarity of each candidate must be above 85%, and the exon deletion number must be less than or equal to 2. After that, all the candidates were blasted against CDS/mRNA database, and a score greater than 80 was determined as a member of MsCCR gene family. Finally, they were confirmed by sequence alignment against the protein database. Regions of resulting signature motifs were identified by a MEGA-X ClustalW sequence alignment, cutoff rate = 30%. If a candidate contains the CCR signature motif "(KNW)YCYGK", it will be named MsCCR, or it will be named MsCCR-like. The pI and MW of amino acids were calculated using ExPASy Compute pI/MW [74].

4.3. Motif Analysis and Gene Structure Visualization

Conserved motifs were found with the widely used online tool Multiple Em for Motif Elicitation (MEME; [75]) [76,77]. Detailed settings are below: motif width is between 6 aa and 50 aa; the maximum motif numbers are set to 20; running under classic model. GSDS online tool [78] was used to visualize exon-intron structure.

4.4. Multiple Sequence Alignment and Phylogenetic Analysis Evolutionary Analysis

The phylogenetic tree was constructed with the neighbor-joining model, JTT method (bootstrap = 400) by MEGA-X [79], and iTOL [80] for decoration. Similarity analysis was conducted through BioEdit [81]. All the sequences used for the phylogenetic tree and alignment are listed in Table S3.

4.5. Cis-regulatory Element Analysis and 3D Structure Prediction

First, 2000 bp upstream was extracted from the initiation codon of each gene to ensure that they contained the promoter region. These sequences were used for cis-regulatory element analysis using PlantCARE [82]. Prediction of the 3D structure was conducted by SWISS-MODEL [83] for modeling (GMQE \geq 0.8) and PyMOL [84] for the exhibition of detailed structure.

4.6. Collinearity Analysis and Chromosome Localization

Collinearity analysis was conducted by TBtools [85] One-step MCScanX, and visualized by TBtools Dual System Plot. Chromosome localization was completed by TBtools Gene Location Visualize from GTF/GFF.

4.7. RNA Isolation and RT-qPCR Analysis

For the total RNA isolation, 500 mg of alfalfa tissues (leaf, stem, and root) under different stages or after different treatments was homogenized and further extracted by using the RNAsiso Plus kit (Takara, Japan, Dalian). Five micrograms of total RNA was used for reverse transcription with the HiScript III 1st Strand cDNA Synthesis Kit (Vazyme, Nanjing, China). qPCR was carried out on an Applied Biosystems™ QuantStudio™ 5 (ABI, Los Angeles, CA, USA). The reaction contains 2 \times ChamQ Universal SYBR qPCR Master Mix (Vazyme, China, Nanjing) 10 μ L, primer F/R (10 μ M) 0.4 μ L, template 200 ng, and

ddH₂O makes up to 20 µL. Relative expression levels were calculated by using the $2^{-\Delta\Delta CT}$ method with *Actin2* used as the internal reference. The primer sequences are listed in Table S4.

4.8. Lignin Content and Staining Analysis

The main stem was sliced by hand and soaked in 2% phloroglucin (in 95% ethanol) for 5 to 10 s, then treated with 12% muriatic acid for 5 to 10 s until lignin turns red. The time was extended to 20 to 30 s when treating the whole root.

4.9. Cloning, Expression, and Purification of Recombinant MsCCR

The target sequences were cloned from the cDNA template. Plasmid *pET-28α* was used to construct the expression vector. Constructed vectors were stored in *Escherichia coli* DH5α. The vector was transferred into *E. coli* BL21 and cultured in Luria–Bertani (LB) medium 37 °C 210 rpm. The recombinant proteins were induced at 16 °C 150 rpm with 200 µM isopropyl-β-D-thiogalactoside (IPTG) in LB medium for at least 5 h or overnight when OD₆₀₀ = 0.6–0.8. Induced BL21 was centrifuged and resuspended in 1 × PBS. The cells were disrupted on ice by a sonic dismembrator with 100 µM phenylmethylsulfonyl fluoride (PMSF). After centrifuging at 8000 rpm 4 °C for 20 min, the liquid was filtered (0.45 µm filter) in BBI™ Ni-NTA 1 mL (Prepacked Gravity Column), then eluted with imidazole of different concentrations (20 mM, 50 mM, 100 mM, 250 mM, or 500 mM) in LE buffer. The His-tagged MsCCR proteins were eluted with 100 mM imidazole. The His-tagged MsCCR proteins were eluted with 100 mM imidazole. The purification of obtained proteins was valued by Western blot using an anti-His tag antibody.

4.10. CCR Activity and Enzyme Kinetic Parameter Analysis

The protein eluted by 100 mM imidazole was dialyzed in 1 × PBS with 1 mM dithiothreitol (DTT), magnetic stirring on ice for 3 h. BCA Protein Assay Kit (Takara, China, Dalian) was used to detect the protein content of dialyzed enzymes. For enzymatic analysis, a 500 µL reaction was used, containing the following content: enzyme 20 µg, NADPH 160 µM, substrate (feruloyl-CoA, *p*-coumaroyl-CoA, caffeoyl-CoA, and sinapoyl-CoA) (ZZBIO CO., LTD, China, Shanghai) 30–150 µM, 1 × PBS to 500 µL. The decrease of A₃₆₆ was recorded, and changed the concentration of different substrates. The parameters K_m , V_{max} , and K_{cat} will be calculated by $V_0/[S] - V_0$ plots.

5. Conclusions

The present study identified 30 CCRs in *M. sativa* genome, and further analyzed the phylogenetics and evolution of CCR family proteins. Seven *MsCCR* genes were located on seven chromosomes in alfalfa, which are homologous to two CCR genes in *M. truncatula*. Meanwhile, 23 *MsCCR-like* genes were categorized into four subfamilies. The expression patterns in alfalfa seedlings at different growth stages suggested that *MsCCR* genes play an important role in cell wall lignification. In addition, both *MsCCR* and *MsCCR-like* genes responded to environmental stresses and hormone treatment, which is consistent with the *cis*-elements in their promoters. Furthermore, the biochemical and three-dimensional structure model analysis of recombinant *MsCCR1* and *MsCCR-like1* suggested the importance of some motifs for catalytic activities under the specific substrates.

Supplementary Materials: The following supporting information can be downloaded at: <https://www.mdpi.com/article/10.3390/ijms23147762/s1>.

Author Contributions: W.C., Z.Z., P.J. and J.P. performed the experiments. W.C., Z.Z. and G.Z. analyzed the data. W.C., S.X. and W.S. drafted and revised the manuscript. W.S. supervised the experiments and the manuscript. All authors have read and agreed to the published version of the manuscript.

Funding: This work was supported by the fund from the National Natural Science Foundation of China (Grant No. 31871545).

Institutional Review Board Statement: Not applicable.

Informed Consent Statement: Not applicable.

Data Availability Statement: All data are contained within the article and supplementary files.

Conflicts of Interest: The authors declare no conflict of interest.

References

1. Prasad, N.; Vindal, V.; Kumar, V.; Kabra, A.; Phogat, N.; Kujmar, M. Structural and docking studies of *Leucaena leucocephala* cinnamoyl CoA reductase. *J. Mol. Model.* **2011**, *17*, 533–541. [[CrossRef](#)]
2. Jung, H.J.G.; Samac, D.A.; Sarath, G. Modifying crops to increase cell wall digestibility. *Plant Sci.* **2012**, *185*, 65–77. [[CrossRef](#)] [[PubMed](#)]
3. Barros, J.; Temple, S.; Dixon, R.A. Development and commercialization of reduced lignin alfalfa. *Curr. Opin. Biotech.* **2019**, *56*, 48–54. [[CrossRef](#)] [[PubMed](#)]
4. Chen, L.; Auh, C.K.; Dowling, P.; Bell, J.; Lehmann, D.; Wang, Z.Y. Transgenic down-regulation of caffeic acid O-methyltransferase (COMT) led to improved digestibility in tall fescue (*Festuca arundinacea*). *Funct. Plant Biol.* **2004**, *31*, 235–245. [[CrossRef](#)] [[PubMed](#)]
5. Grev, A.M.; Hathaway, M.R.; Sheaffer, C.C.; Wells, M.S.; Reiter, A.S.; Martinson, K.L. Apparent digestibility, fecal particle size, and mean retention time of reduced lignin alfalfa hay fed to horses. *J. Anim. Sci.* **2021**, *99*, skab158. [[CrossRef](#)]
6. Reddy, M.S.; Chen, F.; Shadle, G.; Jackson, L.; Aljoe, H.; Dixon, R.A. Targeted down-regulation of cytochrome P450 enzymes for forage quality improvement in alfalfa (*Medicago sativa* L.). *Proc. Natl. Acad. Sci. USA* **2005**, *102*, 16573–16578. [[CrossRef](#)]
7. Carocha, V.; Soler, M.; Hefer, C.; Cassan-Wang, H.; Fevereiro, P.; Myburg, A.A.; Paiva, J.A.P.; Grima-Pettenati, J.G. Genome-wide analysis of the lignin toolbox of *Eucalyptus grandis*. *New Phytol.* **2015**, *206*, 1297–1313. [[CrossRef](#)]
8. Chen, F.; Dixon, R.A. Lignin modification improves fermentable sugar yields for biofuel production. *Nat. Biotechnol.* **2007**, *25*, 759–761. [[CrossRef](#)]
9. Simmons, B.A.; Loqué, D.; Ralph, J. Advances in modifying lignin for enhanced biofuel production. *Curr. Opin. Plant Biol.* **2010**, *13*, 313–320. [[CrossRef](#)]
10. Umezawa, T. Lignin modification *in planta* for valorization. *Phytochem. Rev.* **2018**, *17*, 1305–1327. [[CrossRef](#)]
11. Hisano, H.; Nandakumar, R.; Wang, Z.Y. Genetic modification of lignin biosynthesis for improved biofuel production. *In Vitro Cell. Dev. Biol.* **2009**, *45*, 306–313. [[CrossRef](#)]
12. De Meester, B.; Calderón, B.M.; de Vries, L.; Pollier, J.; Goeminne, G.; Van Doorselaere, J.; Chen, M.; Ralph, J.; Vanholme, R.; Boerjan, W. Tailoring poplar lignin without yield penalty by combining a null and haploinsufficient *CINNAMOYL-CoA REDUCTASE2* allele. *Nat. Commun.* **2020**, *11*, 5020. [[CrossRef](#)] [[PubMed](#)]
13. Vanholme, R.; Demedts, B.; Morreel, K.; Ralph, J.; Boerjan, W. Lignin biosynthesis and structure. *Plant Physiol.* **2010**, *153*, 895–905. [[CrossRef](#)] [[PubMed](#)]
14. Barros, J.; Serk, H.; Granlund, I.; Pesquet, E. The cell biology of lignification in higher plants. *Ann. Bot.* **2015**, *115*, 1053–1074. [[CrossRef](#)] [[PubMed](#)]
15. Jones, L.; Ennos, A.R.; Turner, S.R. Cloning and characterization of *irregular xylem4 (irx4)*: A severely lignin-deficient mutant of *Arabidopsis*. *Plant J.* **2001**, *26*, 205–216. [[CrossRef](#)] [[PubMed](#)]
16. Khakdan, F.; Nasiri, J.; Ranjbar, M.; Alizadeh, H. Water deficit stress fluctuates expression profiles of *4Cl*, *C3H*, *COMT*, *CVOMT* and *EOMT* genes involved in the biosynthesis pathway of volatile phenylpropanoids alongside accumulation of methylchavicol and methyleugenol in different Iranian cultivars of basil. *J. Plant Physiol.* **2017**, *218*, 74–83. [[CrossRef](#)]
17. Ali, M.B.; Singh, N.; Shohael, A.M.; Hahn, E.J.; Paek, K.Y. Phenolics metabolism and lignin synthesis in root suspension cultures of *Panax ginseng* in response to copper stress. *Plant Sci.* **2006**, *171*, 147–154. [[CrossRef](#)]
18. Denness, L.; McKenna, J.F.; Segonzac, C.; Wormit, A.; Madhou, P.; Bennett, M.; Mansfield, J.; Zipfel, C.; Hamann, T. Cell wall damage-induced lignin biosynthesis is regulated by a reactive oxygen species- and jasmonic acid-dependent process in *Arabidopsis*. *Plant Physiol.* **2011**, *156*, 1364–1374. [[CrossRef](#)]
19. Hu, D.; Liu, X.B.; Shen, H.Z.; Gao, Z.; Ruan, R.W.; Wu, D.Q.; Yi, Z.L. The lignin synthesis related genes and lodging resistance of *Fagopyrum esculentum*. *Biol. Plantarum.* **2017**, *61*, 138–146. [[CrossRef](#)]
20. Begović, L.; Abičić, I.; Lalić, A.; Lepeduš, H.; Cesar, V.; Leljok-Levanić, D. Lignin synthesis and accumulation in barley cultivars differing in their resistance to lodging. *Plant Physiol. Biochem.* **2018**, *133*, 142–148. [[CrossRef](#)]
21. Baxter, H.L.; Stewart, N., Jr. Effects of altered lignin biosynthesis on phenylpropanoid metabolism and plant stress. *Biofuels* **2013**, *4*, 635–650. [[CrossRef](#)]
22. Gou, M.; Yang, X.; Zhao, Y.; Ran, X.; Song, Y.; Liu, C.J. Cytochrome *b5* is an obligate electron shuttle protein for syringyl lignin biosynthesis in *Arabidopsis*. *Plant Cell* **2019**, *31*, 1344–1366. [[CrossRef](#)]
23. Zhao, Q.; Dixon, R.A. Transcriptional networks for lignin biosynthesis: More complex than we thought? *Trends Plant Sci.* **2011**, *16*, 227–233. [[CrossRef](#)] [[PubMed](#)]
24. Park, H.L.; Bhoo, S.H.; Kwon, M.; Lee, S.W.; Cho, M.H. Biochemical and expression analyses of the rice cinnamoyl-CoA reductase gene family. *Front. Plant Sci.* **2017**, *8*, 2099. [[CrossRef](#)] [[PubMed](#)]

25. Nakashima, J.; Chen, F.; Jackson, L.; Shadle, G.; Dixon, R. Multi-site genetic modification of monolignols biosynthesis in alfalfa (*Medicago sativa*): Effects on lignin composition in specific cell types. *New Phytol.* **2008**, *179*, 738–750. [[CrossRef](#)] [[PubMed](#)]
26. Tamasloukht, B.; Lam, M.S.-J.W.Q.; Martinez, Y.; Tozo, K.; Barbier, O.; Jourda, C.; Jauneau, A.; Borderies, G.; Balzergue, S.; Renou, J.P.; et al. Characterization of a cinnamoyl-CoA reductase 1 (CCR1) mutant in maize: Effects on lignification, fibre development, and global gene expression. *J. Exp. Bot.* **2011**, *62*, 3837–3848. [[CrossRef](#)]
27. Tu, Y.; Rochfort, S.; Liu, Z.; Ran, Y.; Griffith, M.; Badenhorst, P.; Louie, G.V.; Bowman, M.E.; Smith, K.F.; Noel, J.P.; et al. Functional analyses of *caffeic acid O-methyltransferase* and *cinnamoyl-CoA-reductase* genes from perennial ryegrass (*Lolium perenne*). *Plant Cell* **2010**, *22*, 3357–3373. [[CrossRef](#)]
28. Lauvergeat, V.; Lacomme, C.; Lacombe, E.; Lasserre, E.; Poby, D.; Grima Pettenati, J. Two cinnamoyl-CoA reductase (CCR) genes from *Arabidopsis thaliana* are differentially expressed during development and in response to infection with pathogenic bacteria. *Phytochemistry* **2001**, *57*, 1187–1195. [[CrossRef](#)]
29. Raes, J.; Rohde, A.; Christensen, J.H.; Van de Peer, Y.; Boerjan, W. Genome-wide characterization of the lignification toolbox in *Arabidopsis*. *Plant Physiol.* **2003**, *133*, 1051–1071. [[CrossRef](#)]
30. Thévenin, J.; Pollet, B.; Letarnec, B.; Saulnier, L.; Gissot, L.; Maia-Grondard, A.; Lapierre, C.; Jounanin, L. The simultaneous repression of CCR and CAD, two enzymes of the lignin biosynthetic pathway, results in sterility and dwarfism in *Arabidopsis thaliana*. *Mol. Plant* **2011**, *4*, 70–82. [[CrossRef](#)]
31. De Meester, B.; de Vries, L.; Özparpucu, M.; Gierlinger, N.; Corneillie, S.; Pallidis, A.; Goeminne, G.; Morreel, K.; De Bruyne, M.; De Rycke, R.; et al. Vessel-specific reintroduction of CINNAMOYL-COA REDUCTASE1 (CCR1) in dwarfed *ccr1* mutants restores vessel and xylary fiber integrity and increases biomass. *Plant Physiol.* **2018**, *176*, 611–633. [[CrossRef](#)] [[PubMed](#)]
32. Escamilla-Treviño, L.L.; Shen, H.; Uppalapati, S.R.; Ray, T.; Tang, Y.; Hernandez, T.; Yin, Y.; Xu, Y.; Dixon, R.A. Switchgrass (*Panicum virgatum*) possesses a divergent family of cinnamoyl CoA reductases with distinct biochemical properties. *New Phytol.* **2010**, *185*, 143–155. [[CrossRef](#)] [[PubMed](#)]
33. Shi, R.; Sun, Y.H.; Li, Q.; Heber, S.; Sederoff, R.; Chiang, V.L. Towards a systems approach for lignin biosynthesis in *Populus trichocarpa*: Transcript abundance and specificity of the monolignols biosynthetic genes. *Plant Cell Physiol.* **2010**, *51*, 144–163. [[CrossRef](#)]
34. Zhou, R.; Jackson, L.; Shadle, G.; Nakashima, J.; Temple, S.; Chen, F.; Dixon, R.A. Distinct cinnamoyl CoA reductases involved in parallel routes to lignin in *Medicago truncatula*. *Proc. Natl. Acad. Sci. USA* **2010**, *107*, 17803–17808. [[CrossRef](#)]
35. Borah, P.; Khurana, J.P. The OsFBK1 E3 ligase subunit affects anther and root secondary cell wall thickenings by mediating turnover of a cinnamoyl-CoA reductase. *Plant Physiol.* **2018**, *176*, 2148–2165. [[CrossRef](#)] [[PubMed](#)]
36. Chen, H.; Zeng, Y.; Yang, Y.; Huang, L.; Tang, B.; Zhang, H.; Hao, F.; Liu, Y.; Zhang, X.; Zhang, R.; et al. Allele-aware chromosome-level genome assembly and efficient transgene-free genome editing for the autotetraploid cultivated alfalfa. *Nat. Commun.* **2020**, *11*, 2494. [[CrossRef](#)]
37. The Protein Database from NCBI. Available online: <https://ncbi.nlm.nih.gov/protein> (accessed on 30 April 2021).
38. Chao, N.; Jiang, W.T.; Wang, X.C.; Jiang, X.N.; Gai, Y. Novel motif is capable of determining CCR and CCR-like proteins based on the divergence of CCRs in plants. *Tree Physiol.* **2019**, *39*, 2019–2026. [[CrossRef](#)]
39. Xia, H.; Liu, X.; Lin, Z.; Zhang, X.; Wu, M.; Wang, T.; Deng, H.; Wang, J.; Lin, L.; Deng, Q.; et al. Genome-wide identification of MYB transcription factors and screening of members involved in stress response in *Actinidia*. *Int. J. Mol. Sci.* **2022**, *23*, 2323. [[CrossRef](#)]
40. Beckers, B.; De Beek, M.O.; Weyens, N.; Van Acker, R.; Van Montagu, M.; Boerjan, W.; Vangronsveld, J. Lignin engineering in field-grown polar trees affects the endosphere bacterial microbiome. *Proc. Natl. Acad. Sci. USA* **2016**, *113*, 2312–2317. [[CrossRef](#)]
41. Halpin, C. Lignin engineering to improve saccharification and digestibility in grasses. *Curr. Opin. Biotechnol.* **2019**, *56*, 223–229. [[CrossRef](#)]
42. Wang, H.; Yang, J.H.; Chen, F.; Torres-Jerez, I.; Tang, Y.; Wang, M.; Du, Q.; Cheng, X.; Wen, J.; Dixon, R. Transcriptome analysis of secondary cell wall development in *Medicago truncatula*. *BMC Genomics* **2016**, *17*, 23. [[CrossRef](#)] [[PubMed](#)]
43. Costa, M.A.; Collins, R.E.; Anterola, A.M.; Cochrane, F.C.; Davin, L.B.; Lewis, N.G. An in silico assessment of gene function and organization of the phenylpropanoid pathway metabolic networks in *Arabidopsis thaliana* and limitations thereof. *Phytochemistry* **2003**, *64*, 1097–1112. [[CrossRef](#)]
44. Chao, N.; Li, N.; Qi, Q.; Li, S.; Lv, S.; Jiang, X.N.; Gai, Y. Characterization of the cinnamoyl-CoA reductase (CCR) gene family in *Populus tomentosa* reveals the enzymatic active sites and evolution of CCR. *Planta* **2017**, *245*, 61–75. [[CrossRef](#)] [[PubMed](#)]
45. Su, X.; Zhao, Y.; Wang, H.; Li, G.; Cheng, X.; Jin, Q.; Cai, Y. Transcriptomic analysis of early fruit development in Chinese white pear (*Pyrus bretschneideri* Rehd.) and functional identification of *PbCCR1* in lignin biosynthesis. *BMC Plant Biol.* **2019**, *19*, 417. [[CrossRef](#)] [[PubMed](#)]
46. Wang, X.; Niu, Y.; Zheng, Y. Multiple functions of MYB transcription factors in abiotic stress responses. *Int. J. Mol. Sci.* **2021**, *22*, 6125. [[CrossRef](#)] [[PubMed](#)]
47. Xiao, R.; Zhang, C.; Guo, X.; Li, H.; Lu, H. MYB transcription factors and its regulation in secondary cell wall formation and lignin biosynthesis during xylem development. *Int. J. Mol. Sci.* **2021**, *22*, 3560. [[CrossRef](#)] [[PubMed](#)]
48. Song, Z.; Wang, D.; Gao, Y.; Li, C.; Jiang, H.; Zhu, X.; Zhang, H. Changes of lignin biosynthesis in tobacco leaves during maturation. *Funct. Plant Biol.* **2021**, *48*, 624–633. [[CrossRef](#)]

49. Wang, Y.X.; Teng, R.M.; Wang, W.L.; Wang, Y.; Shen, W.; Zhuang, J. Identification of genes revealed differential expression profiles and lignin accumulation during leaf and stem development in tea plant (*Camellia sinensis* (L.) O. Kuntze). *Protoplasma* **2019**, *256*, 359–370. [[CrossRef](#)]
50. Yoon, J.; Choi, H.; An, G. Roles of lignin biosynthesis and regulatory genes in plant development. *J. Integr. Plant Biol.* **2015**, *57*, 902–912. [[CrossRef](#)]
51. Rao, X.; Chen, X.; Shen, H.; Ma, Q.; Li, G.; Tang, Y.; Pena, M.; York, W.; Frazier, T.P.; Lenaghan, S.; et al. Gene regulatory networks for lignin biosynthesis in switchgrass (*Panicum virgatum*). *Plant Biotechnol. J.* **2019**, *17*, 580–593. [[CrossRef](#)]
52. Cheng, X.; Li, M.; Li, D.; Zhang, J.; Jin, Q.; Sheng, L.; Cai, Y.; Lin, Y. Characterization and analysis of CCR and CAD gene families at the whole-genome level for lignin synthesis of stone cells in pear (*Pyrus bretschneideri*) fruit. *Biol. Open* **2017**, *6*, 1602–1613. [[CrossRef](#)] [[PubMed](#)]
53. Wei, S.; Wang, L.; Zhang, Y.; Huang, D. Identification of early response genes to salt stress in roots of melon (*Cucumis melo* L.) seedlings. *Mol. Biol. Rep.* **2013**, *40*, 2915–2926. [[CrossRef](#)] [[PubMed](#)]
54. Hori, C.; Yu, X.; Mortimer, J.C.; Sano, R.; Matsumoto, T.; Kikuchi, J.; Demura, T.; Ohtani, M. Impact of abiotic stress on the regulation of cell wall biosynthesis in *Populus trichocarpa*. *Plant Biotech.* **2020**, *37*, 273–283. [[CrossRef](#)] [[PubMed](#)]
55. Liu, D.; Wu, J.; Lin, L.; Li, P.; Wang, Y.; Li, J.; Sun, Q.; Liang, J.; Wang, Y. Overexpression of cinnamoyl-CoA reductase 2 in *Brassica napus* increases resistance to *sclerotinia sclerotiorum* by affecting lignin biosynthesis. *Front. Plant Sci.* **2021**, *12*, 732733. [[CrossRef](#)] [[PubMed](#)]
56. Bang, S.W.; Choi, S.; Jin, X.; Jung, S.E.; Choi, J.W.; Seo, J.S.; Kim, J.K. Transcriptional activation of rice *CINNAMOYL-CoA REDUCTASE 10* by OsNAC5, contributes to drought tolerance by modulating lignin accumulation in roots. *Plant Biotechnol. J.* **2022**, *20*, 736–747. [[CrossRef](#)] [[PubMed](#)]
57. Barakat, A.; Yassin, N.B.M.; Park, J.S.; Choi, A.; Herr, J.; Carlson, J.E. Comparative and phylogenomic analyses of cinnamoyl-CoA reductase and cinnamoyl-CoA-reductase-like gene family in land plants. *Plant Sci.* **2011**, *181*, 249–257. [[CrossRef](#)] [[PubMed](#)]
58. Ma, R.; Xio, Y.; Lv, Z.; Tan, H.; Chen, R.; Li, Q.; Chen, J.; Wang, Y.; Yin, J.; Zhang, L.; et al. AP2/ERF transcription factor, *li049*, positively regulates lignin biosynthesis in *Isatic indigotica* through activating salicylic acid signaling and lignin/lignin pathway genes. *Front. Plant Sci.* **2017**, *8*, 1361. [[CrossRef](#)]
59. Li, M.; Cheng, C.; Zhang, X.; Zhou, S.; Wang, C.; Ma, C.; Yang, S. *PpNAC187* enhances lignin synthesis in “Whangkeumbae” pear (*Pyrus pyrifolia*) “Hard-End” Fruit. *Molecules* **2019**, *24*, 4338. [[CrossRef](#)]
60. Villarreal, N.M.; Marina, M.; Nardi, C.F.; Civello, P.M.; Martínez, G.A. Novel insights of ethylene role in strawberry cell wall metabolism. *Plant Sci.* **2016**, *252*, 1–11. [[CrossRef](#)]
61. Lan, Y.; Chai, Y.; Xing, C.; Wu, K.; Wang, L.; Cai, M. Nitric oxide reduces the aluminum-binding capacity in rice root tips by regulating the cell wall composition and enhancing antioxidant enzymes. *Ecotoxicol. Environ. Saf.* **2021**, *208*, 111499. [[CrossRef](#)]
62. Lacombe, E.; Hawkins, S.; Doorselaere, J.; Piquemal, J.; Goffner, D.; Poeydomenge, O.; Boudet, A.M.; Grima-Pettenati, J. Cinnamoyl CoA reductase, the first committed enzyme of the lignin branch biosynthetic pathway: Cloning, expression and phylogenetic relationships. *Plant J.* **1997**, *11*, 429–441. [[CrossRef](#)] [[PubMed](#)]
63. Baltas, M.; Lapeyre, C.; Bedos-Belval, F.; Maturano, M.; Saint-Aguet, P.; Roussel, L.; Duran, H.; Grima-Pettenati, J. Kinetic and inhibition studies of cinnamoyl-CoA reductase 1 from *Arabidopsis thaliana*. *Plant Physiol. Biochem.* **2005**, *43*, 746–753. [[CrossRef](#)] [[PubMed](#)]
64. Pan, H.; Zhou, R.; Louie, G.V.; Mühlemann, J.K.; Bomati, E.K.; Bowman, M.E.; Dudareva, N.; Dixon, R.A.; Noel, J.P.; Wang, X. Structural studies of cinnamoyl-CoA reductase and cinnamyl-alcohol dehydrogenase, key enzymes of monolignol biosynthesis. *Plant Cell.* **2014**, *26*, 3709–3727. [[CrossRef](#)] [[PubMed](#)]
65. Bart, R.S.; Chern, M.; Vega-Sánchez, M.E.; Canlas, P.; Ronald, P.C. Rice *Snl6*, a cinnamoyl-CoA reductase-like gene family member, is required for NH1-mediated immunity to *Xanthomonas oryzae* pv. *oryzae*. *PLoS Genet.* **2010**, *6*, e1001123. [[CrossRef](#)]
66. Cui, W.; Yao, P.; Pan, J.; Dai, C.; Cao, H.; Chen, Z.; Zhang, S.; Xu, S.; Shen, W. Transcriptome analysis reveals insight into molecular hydrogen-induced cadmium tolerance in alfalfa: The prominent role of sulfur and (homo)glutathione metabolism. *BMC Plant Biol.* **2020**, *20*, 58. [[CrossRef](#)]
67. Hdira, S.; Haddoudi, L.; Hanana, M.; Romero, I.; Mahjoub, A.; Ben Jouira, H.; Ludidi, N.; Sanchez-Ballesta, M.T.; Abdelly, C.; Badri, M. Morpho-Physiological, Biochemical, and Genetic Responses to Salinity in *Medicago truncatula*. *Plants* **2021**, *10*, 808. [[CrossRef](#)]
68. Chen, T.; Yang, Q.; Zhang, X.; Ding, W.; Gruber, M. An alfalfa (*Medicago sativa* L.) ethylene response factor gene, *MsERF11*, enhances salt tolerance in transgenic *Arabidopsis*. *Plant Cell Rep.* **2012**, *31*, 1737–1746. [[CrossRef](#)]
69. Chen, M.; Cui, W.; Zhu, K.; Xie, Y.; Zhang, C.; Shen, W. Hydrogen-rich water alleviates aluminum-induced inhibition of root elongation in alfalfa via decreasing nitric oxide production. *J. Hazard. Mater.* **2014**, *267*, 40–47. [[CrossRef](#)]
70. Xie, Y.; Zhang, W.; Duan, X.; Dai, C.; Zhang, Y.; Cui, W.; Wang, R.; Shen, W. Hydrogen-rich water-alleviated ultraviolet-B-triggered oxidative damage is partially associated with the manipulation of the metabolism of (iso)flavonoids and antioxidant defence in *Medicago sativa*. *Funct. Plant Biol.* **2015**, *42*, 1141–1157. [[CrossRef](#)]
71. Dražić, G.; Mihailović, N.; Lojić, M. Cadmium accumulation in *Medicago sativa* seedlings treated with salicylic acid. *Biol. Plant.* **2006**, *50*, 239–244. [[CrossRef](#)]
72. Kato-Noguchi, H. Abscisic acid increases anaerobic tolerance in alfalfa seedlings. *Physiol. Plantarum* **1999**, *107*, 395–398. [[CrossRef](#)]

73. The Alfalfa (*M. sativa* L.) Genomic Data Base. Available online: https://figshare.com/projects/whole_genome_sequencing_and_assembly_of_Medicago_sativa/66380 (accessed on 20 March 2021).
74. The ExPASy Compute pI/MW Tool. Available online: <https://www.expasy.org/resources/compute-pi-mw> (accessed on 26 April 2021).
75. The Multiple Em for Motif Elicitation Tool. Available online: <http://meme-suite.org> (accessed on 26 April 2021).
76. Hossain, M.S.; Ahmed, B.; Ullah, M.W.; Haque, M.S.; Islam, M.S. Genome-wide identification and characterization of expansin genes in jute. *Trop. Plant Biol.* **2022**, *15*, 40–54. [[CrossRef](#)]
77. Chakraborty, A.; Viswanath, A.; Malipatil, R.; Semalaisyappan, J.; Shah, P.; Ronanki, S.; Rathore, A.; Singh, S.P.; Govindaraj, M.; Tonapi, V.A.; et al. Identification of candidate genes regulating drought tolerance in *Pearl Millet*. *Int. J. Mol. Sci.* **2022**, *23*, 6907. [[CrossRef](#)] [[PubMed](#)]
78. The GSDS Tool. Available online: <http://gsds.cbi.pku.edu.cn/> (accessed on 26 April 2021).
79. The MEGA-X Tool. Available online: <https://www.megasoftware.net/> (accessed on 30 April 2021).
80. The iTOL Software. Available online: <https://itol.embl.de/> (accessed on 16 May 2022).
81. The BioEdit Software. Available online: https://www.nucleics.com/DNA_sequencing_support/Trace_viewer_reviews/BioEdit (accessed on 26 April 2021).
82. The PlantCARE Tool. Available online: <https://bioinformatics.psb.ugent.be/webtools/plantcare/html/> (accessed on 11 May 2021).
83. The SWISS-MODEL Tool. Available online: <https://swissmodel.expasy.org/> (accessed on 29 April 2021).
84. The PyMOL Tool. Available online: <https://pymol.org/2/> (accessed on 12 May 2022).
85. The TBtools. Available online: <https://github.com/CJ-Chen/TBtools/releases> (accessed on 12 May 2022).